ARTICLE IN PRESS

Journal of Petroleum Science and Engineering xxx (xxxx) xxx

Contents lists available at ScienceDirect

Journal of Petroleum Science and Engineering

journal homepage: www.elsevier.com/locate/petrol

A comprehensive perspective on pore connectivity and natural fracture analysis in Oligo-Miocene heterogeneous carbonates, southern Iran

Shervin Bahramali Asadi Kelishami [a], Reza Mohebian [b,*], Omidreza Salmian [b]

[a] *Kish Petroleum Engineering Company (KPE), Tehran, 1958963111, Iran*
[b] *School of Mining Engineering, College of Engineering, University of Tehran, Tehran, Iran*

ARTICLE INFO

Keywords:
Pore connectivity
Permeability
Fracture aperture
Artificial neural network (ANN)
Porosity
Image log
Velocity deviation log (VDL)

ABSTRACT

Ascertaining the pore connection criterion has always been a challenge for geoscientists. In the framework of this research, an attempt was made to study the pore connectivity in a heterogeneous carbonate rock by combining several techniques. Pore types and rock facies were investigated for 321 thin sections. The abundance of connected porosities, cementation type and intensity which significantly control the matrix pore connectivity were specified on thin sections and finally a connectivity log was extracted that showed an accurate result on poro-perm cross-plots. Most of the porosity volumes were related to interparticle, vuggy and moldic porosities which are microscale. The velocity deviation log, estimated in four wells, indicates the presence of micro-porosity, which is consistent with the results of thin-sections. Zero velocity deviation is usually associated with the predominant presence of micro-pores. Different permeability values in identical lithological facies, as well as micro-fracture markers, prompted us to conduct more extensive research on fractures. FMI analysis proved that the studied reservoir is intensively fractured. The recorded high permeability in a sample with low matrix connectivity is specifically a fracture indication. Fracture apertures vary from microscale (<50 μm) to 12.5 mm and calculated fracture density is raised up to 2 fractures per meter. Determined fractured intervals are very consistent with mud-loss information, for instance, a complete loss has been reported in the fault zone identified in well B. The detected fractures somewhat follow the main Zagros fault trend (NW-SE). Eventually, calculated connectivity was predicted in other wells using Artificial Neural Network (ANN) and a 3D model was constructed with respect to seismic attributes which gives a precise perspective of pore connection distribution throughout the studied field.

1. Introduction

Reservoir quality of carbonate rocks is extremely dependent on regional diagenesis and other secondary processes like fractures and micro-fractures. The properties of these reservoirs considerably change both laterally and vertically (Tavakoli, 2019). Heterogeneity is manifested by the presence of different types, sizes, and shapes of pores resulting from sedimentation and diagenetic events (Lima et al., 2020). The rock electrical parameters (m, n) also vary by change in diagenetic facies (Zhou et al., 2019). Sedimentary environment, diagenesis and tectonic are the three substantial factors which control the reservoir quality in such Formations. In the framework of this study, a comprehensive investigation has been carried out based on the performance of Iran's Oligo-Miocene carbonates as a hydrocarbon reservoir Formation. Rock's origin plays an essential role in pore type distribution along with secondary processes. Primary interparticle porosity is usually formed by deposition of a well-sorted calcareous grains under the influence of strong currents or waves or by local production of calcareous sand-size particles with sufficient rapidity to deposit particle on particle with little or no interstitial mud. Dissolution of interstitial mud can produce a micro-vuggy porosity resembling interparticle pore space. Simple cementation by calcite, anhydrite, dolomite, or quartz destroys porosity and pore size (Raymond Carl, 1960). Complex porosity system causes unpredictable hydraulic behavior in such reservoirs. Unlike most sandstone samples, which typically are single-porosity systems, reservoirs in carbonate rocks mostly include multiple porosity systems that characteristically impart petrophysical heterogeneity to the reservoirs (Mazzulo et al., 2004). Heterogeneity in carbonate rocks makes it difficult to anticipate a definite relationship between pore values and production. In some cases, permeability-for-given-porosity is controlled by grain size

* Corresponding author.
E-mail addresses: shervinpn@yahoo.com (S. Bahramali Asadi Kelishami), mohebian@ut.ac.ir (R. Mohebian), omidrezasalmian@ut.ac.ir (O. Salmian).

https://doi.org/10.1016/j.petrol.2021.109199
Received 17 January 2021; Received in revised form 31 May 2021; Accepted 2 July 2021
Available online 8 July 2021
0920-4105/© 2021 Published by Elsevier B.V.

Please cite this article as: Shervin Bahramali Asadi Kelishami, *Journal of Petroleum Science and Engineering*, https://doi.org/10.1016/j.petrol.2021.109199

Table 1
Classification of mud loss severity (Cook et al., 2011).

Mud Loss	Loss Intensity (BBL/Hour)
Seepage	Less than 10
Partial loss	10 to 100
Severe loss	Greater than 100
Total loss	No fluid returns to the surface

Table 2
Table shows mud-loss data reported in well B and calculated fracture density against each interval.

Depth Range (meters)	Mud-loss (BBL/Day)	Fracture Density (n/meter)
2319–2323	850 BBL/Day	2
2363–2440	44 BBL/Day	1.06
2474–2481	650 BBL/Day	1
2481–2485	1800 BBL/Day (Complete loss)	1.5
2496–2503	55 BBL/Day	0.5

and calcite cement content. However, dolomitization may tend to reduce the variation of permeability-for-given-porosity by recrystallizing mud matrix to form intercrystalline macro-porosity that connects vugs and moulds to become integrated with the effective pore system (Ehrenberg et al., 2006). In such cases, it is not usual to encounter sharp differences in permeability–porosity trends for different carbonate textures. In contrast, according to another study implemented on micritic carbonates, samples characterized by a high micrite content were found to have a low permeability at any given porosity. When macro pores are added to the micrite aggregates, permeability rises dramatically with the increase of porosity (El Husseiny et al., 2017). Along with all mentioned items, some phenomena such as cementation intensity, cement types, dissolution intensity, fracture types and distribution, clay volume and also pore types (Isolated and connected pores), are the main factors controlling a carbonate reservoir quality. Although porosity value is a necessary aspect to estimate producible reserve, types of pores possess their own particular importance. A study performed by Wang (Wang et al., 2020) on a tight sandstone reservoir by integrating mercury intrusion porosimetry (MIP), nuclear magnetic resonance (NMR) and scanning electron microscopy (SEM) made it clear that connectivity percentages of pores with different radii (<50 nm, 50 nm–0.1 μm, and 0.1μm–1μm) are not similar. It was found that small pores contributed 5.02%–18.00% to connectivity, which is less than large pores ($r > 0:05$ μm) with contribution of 36.60%–92.00%, although small pores had higher pore volumes. In the framework of this study, effectiveness of pore types has been analyzed through Oligo-Miocene carbonates. Overall, pore types can be segregated into two parts, non-low connected pore types and highly connected pore types. Intergranular, intercrystalline, and fractures usually belong to connected pores group and in contrast, intraparticle, vuggy, moldic and micro porosities are mostly associated with isolated porosities. Open fractures not only can enhance the effective porosity by themselves but also they may link other isolated pores. (see Tables 1 and 2)

2. Geological overview

Southern Iran is considered as one of the most hydrocarbon potential areas in the world. Extension of the massive reservoir and source rocks accompanying with proper cap rocks formed a suitable hydrocarbon system across the area. Along with all the mentioned items, an active tectonic system results in developing numerous anticlinal hydrocarbon traps. The Zagros structure along the eastern margin of Arabian Plate, expands from Turkey in the NW to the Hormuz strait in the SE of Iran (Alavi, 2004a, b). The geodynamic evolution of this fold-thrust belt is mostly linked to opening (late Permian) and closure (late Cretaceous to Neogene) of the Neo-Tethys Ocean (Stampfli et al., 1991; Heydari, 2008). Many tectonic units have been defined within the Zagros structure. The High Zagros is conventionally shown as being bounded to the southwest by the High Zagros Fault, a SW-directed thrust. The other main tectonic unit is the Folded Belt. It is apparent from the High Zagros fault to the Persian Gulf, or to the frontal structures of the Zagros. Many sub-faults are also observed in this region in line with the main Zagros fault (NW-SE trend). The Zagros structure is usually characterized by erosion down to Cretaceous or Oligocene–Miocene carbonates in the prominent whaleback anticlines that are striking geomorphic expressions (Berberian, 1995). The Oligo-Miocene carbonates (Asmari Formation) are exposed at Zagros foreland basin with approximately 206 m thickness comprising of thin, medium and thick to massive bedded carbonates (Allahkarampour et al., 2010). Various factors control rock property and its interaction against fluid types. Geological processes, after and during the sedimentation, directly control reservoir rock properties; especially, diagenesis in carbonate rocks (Kelishami et al., 2021) or possible secondary fractures.

3. Materials and methods

Porosity is one of the most important properties of a reservoir rock but when it comes to production, the issue of Pore Connectivity is raised. Although high connected pore types play significant role in reservoir quality level, the effects of clay mineral types and values cannot be ignored. Clay minerals like Illite and Kaolinite may directly affect the reservoir quality by blocking pore throats and filling free spaces. For an accurate estimation of connectivity distribution, it is essential to choose a multidimensional study. Integrating core data, petrophysical well logs, geophysical standpoint and thin section microscopy analysis can provide a befitting overview of the reservoir formation properties over a hydrocarbon field. A study performed by Tonietto (Tonietto et al., 2014) focusing on thin section sample connectivity offered an equation for Connectivity coefficient. Pore connectivity data come from the definition of pore types, pore size distribution, patchiness (spatial distribution of pores), and characteristics of cementation, dolomitization and dissolution processes. Giving values to each of these textural characteristics, a numerical result also is generated through an equation, which gives information about pore connectivity (Tonietto et al., 2014).

$$\text{Connectivity coefficient} = \text{Porosity} * \text{Macro} - \text{porosity (in fraction)} * \text{Pore type combination} * \text{Dissolution intensity} * \text{Cement type (s)} * \text{Cementation intensity} * (9/19.5) + 1$$

According to the mentioned study, 6 different components were considered as major effective factors controlling the connectivity grade, including percentage of porosity, distribution of macro-porosities, pore types (isolated/connected), cement type (rimming/meniscus) and intensity (cementation percentage of each sample), and dissolution grade.

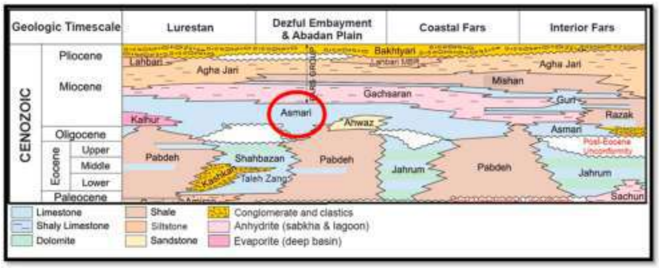

Fig. 1. Cenozoic stratigraphic correlation chart of the Iranian sector of the Zagros basin (James and Wynd, 1965).

Although the offered method by Tonietto may be functional for the estimation of rock matrix connectivity, it may not completely include some other features like macro-fractures effect on total connectivity and permeability. It is also limited to the area that thin section samples were provided. We have estimated the whole interval connectivity with respect to available well logs. In addition, we integrated the thin section extracted connectivity with fracture analysis results and velocity deviation log (VDL) to get an accurate understanding of the reason of permeability and production strength and weakness in the studied Oligo-Miocene carbonates. Thin section study does not cover macro-scale features like major fractures and possible faults which are effective in hydrocarbon production and rock's connectivity. For instance, sometimes, we encounter high permeability in an interval with low matrix connectivity. This study made it obvious that the reason is the available open fractures detected by image log analysis.

In the current study, due to the dominance of micro-pores (<50 μm) in the Oligo-Miocene samples, Macro-porosity (>50 μm) factor has ignored from the equation. Thin section information, sometimes, does not imply on whole interval content, due to the limitation in the expanse of plug sample. Thus, supplementary information and studies are needed to get the most reliable outcomes. Therefore, Formation image log analysis as well as velocity deviation log (VDL) estimation is added to the procedure to combine with the thin section study results. 321 thin section samples have been taken into account in the current study to obtain the matrix connectivity coefficient throughout the Oligo-Miocene carbonate formation. Core plugs sampling rate were 0.3 m and due to the bad core recovery, some of the intervals do not include core samples. Hence, Artificial Neural Network method (ANN) was utilized to fill out the gaps and estimate a continuous connectivity log. Conventional well logs such as Bulk density (RHOB), Neutron porosity (NPHI), Computed gamma ray (CGR), Photo electric factor (PEF), Sonic log (DT), Deep Laterolog (LLD) and Micro spherical focused log were the main data which participated in ANN propagation.

In accordance with the effects of the tectonic system on reservoir rocks, it was necessary to combine the aforementioned work steps with a focused study on potentially related fractures. Thus, evaluation of FMI (Formation Micro-Imager log) and fracture analysis were added to the research program. Eventually, a 3D model of pore connectivity is constructed using seismic attributes with respect to predicted connectivity

Fig. 2. The satellite map illustrating the location of the studied area (Google, 2020).

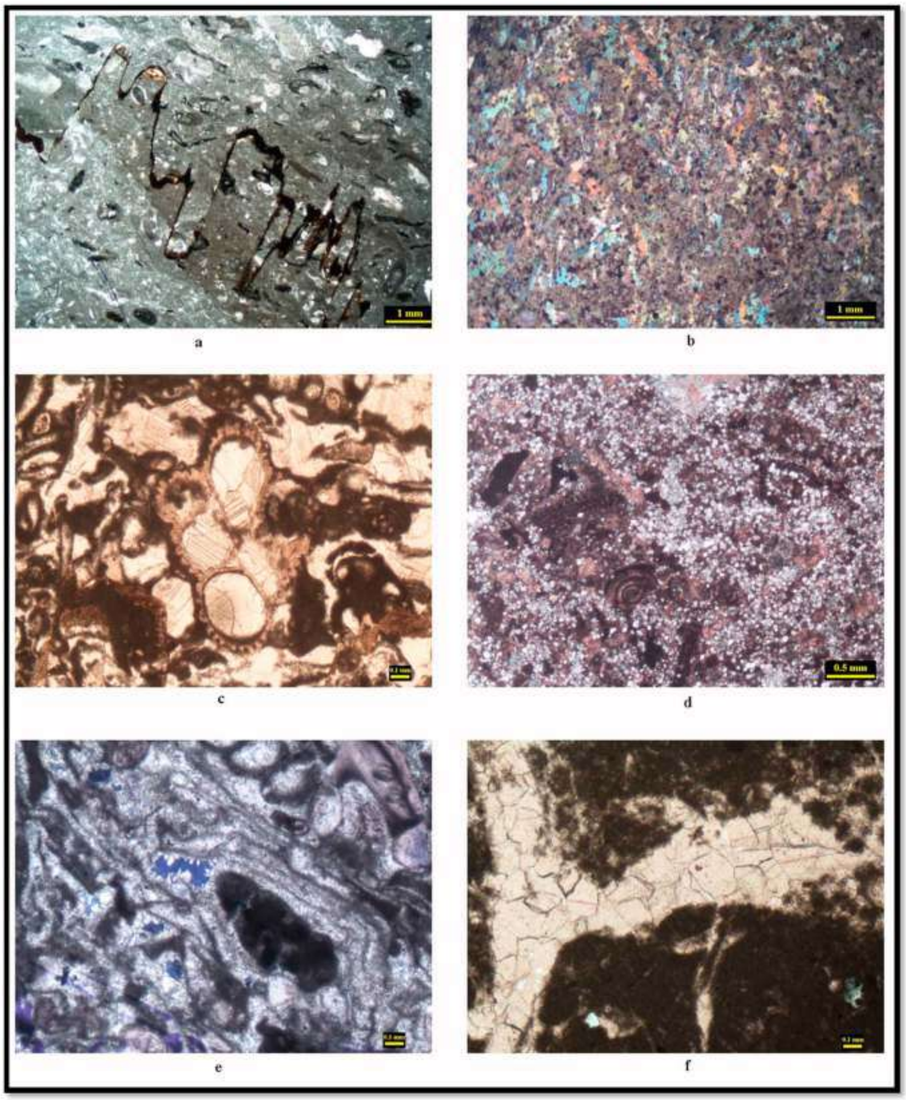

Fig. 3. a: Stylolite formation as a result of compaction process in Oligo-Miocene carbonates. b: Filling pore spaces with Anhydrite cement. c: High-intensity calcite cement blocking pore spaces, compaction effect is obviously observed on grains. d: Available porosity filled by dolomite cement arising from Mg-rich subsurface fluids. e & f: Rimming and meniscus pore-blocking carbonate cements.

data.

Multi-attribute seismic analysis is a broad term that utilizes more than one attribute to predict the earth's physical property. The integration of well-log and seismic data has been a consistent aim of geoscientists (Hampson, 2001). The prediction of reservoir properties is one of the most feasible approaches for determining new exploration/production objects, selecting an optimal exploration and exploitation program, improving the success ratio of drilling, and finally improving the exploration economic benefit (see Figs. 1 and 2).

4. Core samples description

321 thin section samples were provided from available core plugs and aimed at pore type analysis and diagenetic events affecting rock properties. Pore connectivity is the pivotal factor in the current thin section study and the possible impacts on pore connection can arise from some substantial elements including cement types, cement intensity, pore types (connected/isolated) and dissolution intensity. In the studied area, Oligo-Miocene carbonates had highly exposed to cementation and it is an inextricable factor which impacted reservoir properties (Fig. 3). Cement mineral types were mostly comprised of anhydrite, calcite and dolomites which appeared in different cementation forms including rimming, meniscus and pore blocking. Along with cementation, some other processes such as compaction had drastically affected rock properties by closing pore spaces. Abundance of stylolites in plug samples is a great evidence of the compaction effect on rock samples (Fig. 3-a). Dolomitization is another factor which had affected the pore space and connection. As shown in the figure below (Fig. 3-d), an intense invasion of Mg-rich subsurface fluids was led to local increase in dolomite crystallization. Dolomtization process can be considered both destructive and constructive. This process was filled the available free spaces and reduced the matrix porosity in the studied carbonate rocks. In

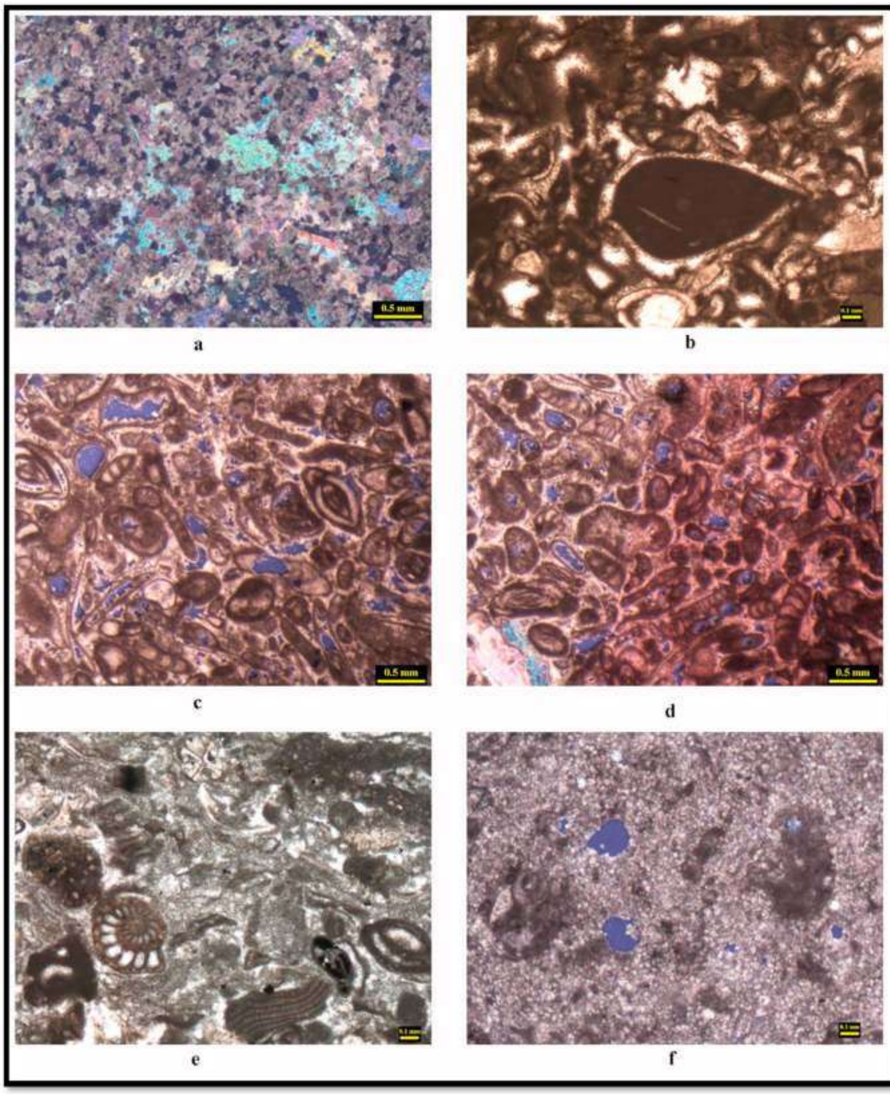

Fig. 4. a: Inter-crystalline pores under the effect of anhydrite cement. b & c & d: Inter-granular, mouldic and intra-granular pore types in allochemical grainstone-packstone facies. e: Micrite is recrystallized into sparry calcite and sparite. Abundance of intra-granular and vuggy porosities are also observed.

additionally to the above, in some cases, anhydrite cement blocked all free spaces and decreased the matrix porosity level to zero (Fig. 3-b). As a result of thin section studies carried out in this field, it is concluded that the matrix porosity was highly under the influence of reductive factors such as cementation and compaction and this is the reason why porosity percentage recorded by well-logs and thin sections does not exceed 8%. Pore types identified in available samples vary depending on sedimentary environments and diagenetic events. Grainstones, packstones, wackestone and mudstone facies are widely scattered in these rocks. The dominant type of pores is related to isolated pores such as intragranular, vuggy and micropores. In some cases, dolomitization causes the formation of local intercrystalline porosities but they sporadically affected by secondary replacing cements (Fig. 4-a). Although inter-granular porosities are the most abundant connected pores recognized in the studied rocks, their distribution is highly limited. Inter-granular pores usually appeared in some specific zones which consist of grainstones and packstones. In addition to inter-granular pores, micro fractures are widely observed throughout the Oligo-Miocene formation. We can divide them into two types, those are filled by cement (mostly carbonate cement) and those which are considered as open micro-fractures and can participate in the production process (Fig. 5). In the present survey, fractures with aperture width lower than 50 micro-meters considered as micro-fractures. Although all such micro-fractures are not easily recognizable in FMI, they were simply identified on thin sections. As mentioned in Schlumberger wireline services catalog, fine details greater than 0.002-in (0.051 mm) wide fractures filled with conductive fluids are visible in images from the FMI imager (Schlumberger, 2015).

Connectivity log was calculated based on 321 available thin sections and plotted (as color) on Poro-Perm standard cross-plot (Fig. 6). Generally, the range of connectivity log is between 1 and 10. The grade of 10 belongs to a sample containing dominant connected pores accompanying with highest level of available porosity which does not expose cementation. Owing to the abundance of isolated pores and the high percentage of cementation, in the scale of this study, we have not encountered the connectivity over grade 5. Connectivity log was calculated based on available thin sections of 2 wells and presented on figures below.

5. velocity deviation log

To investigate the validity and distribution of pore types, Velocity

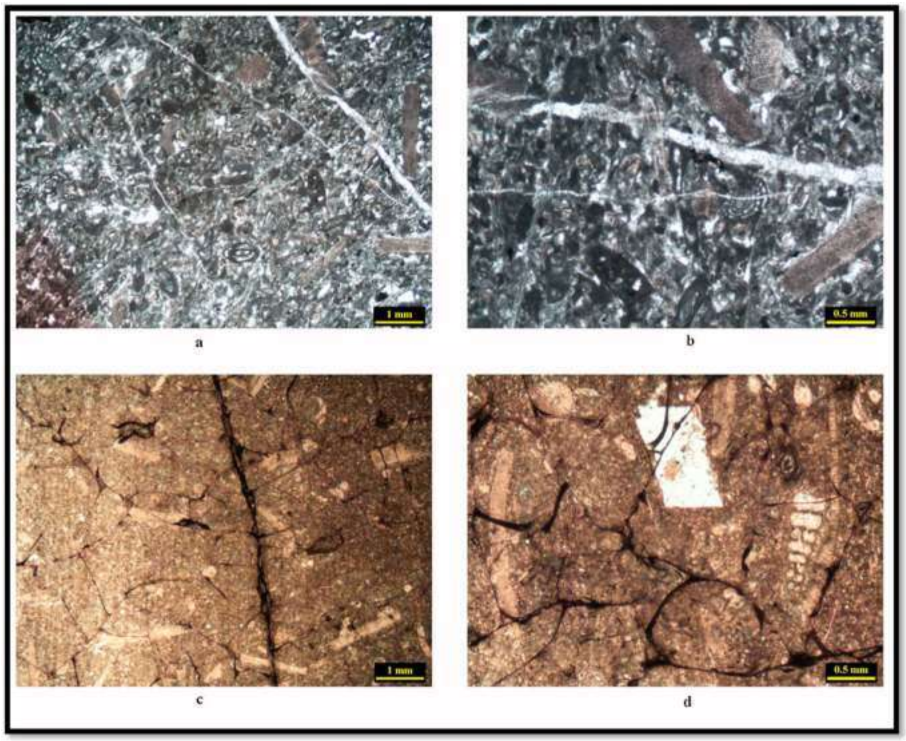

Fig. 5. Figures a and b are showing closed micro-fractures which filled with calcite cement. Figures c and d are the great evidence of available open micro-fractures formed in Oligo-Miocene carbonate rocks.

Deviation Log (VDL) was also estimated in some available wells. It is calculated by combining the sonic log with the neutron-density porosity, provides a tool to achieve downhole information on the predominant pore type in carbonates (Anselmetti et al., 1999). Positive velocity deviations mark zones where velocity is higher than expected from the porosity values (V>+500 m/s), such as zones where frame-forming pore types dominate. Zero deviations (−500 < V<+500) show intervals where the rock lacks a rigid frame, such as in carbonates with high interparticle porosity or micro porosity. Negative deviations mark zones in which sonic log's velocity is unusually low. For instance, cavernous borehole walls, Shales or fracturing can be the reasons (Anselmetti et al., 1999). The VDL log is usually shown in the scale of meters per second (M/S) and its sampling rate in this study is 0.1524 m. By making a correlation between the results of thin section analysis and VDL, it was found that micro-pores dominantly control the porosity volume of the Oligo-Miocene carbonate rocks. As shown in Fig. 7, zero deviations are significantly observed and they were visually verified by thin section samples as well. Although pore types observed on core samples are mixed, a major part of them is in micro scale (isolated micro-pore) and this is the reason why matrix permeability is too low.

6. Image log analysis

Results of both VDL and core samples made it clear that the sporadic increase in permeability in studied carbonates would not relate to matrix properties. Significant increase in permeability in samples with zero porosity which is obvious on Poro-Perm cross-plots specify another enhancing factor that made us analyze the formation micro-imager log data. Natural close and open fracture analysis was the main issue in this part. To do so, the image log of well B was evaluated. As it is obvious in Fig. 8, image log analysis proved a pervasive fracturing in the studied reservoir intervals. Fracture density is extremely raised in some intervals, for instance, it reaches its peak by 5 fractures per meter and it reveals that the studied field was highly exposed to an active tectonic system. Trends of detected natural fractures are mostly NW-SE and follow the main Zagros thrust belt trend (Fig. 10). It is worth mentioning that NW-SE (Zagros trend) and N–S-NE-SW (Arabian trend) are the general trends of most hydrocarbon fields in SW Iran (Alavi, 2004a, b). The detected fault in image analysis is very consistent with Zagros trend and its existence verified by three different indications such as mud loss information (complete loss), zero velocity deviation (<-500) and mudcake data recorded by caliper tool (Fig. 9). A significant declination is also observed between the beddings located in top and the bottom of the detected fault. When drilling fluids enter the formation through fractures, faults or caverns at a rate more than 100 bbl/hour, the losses are classified as severe (Cook et al., 2011). These include total losses, in which no volume of drilling mud makes the return trip to the surface (Cook et al., 2011).

Image analysis results showed that intervals which were under the effect of dolomitization are less lucky to be fractured. Fracture density log is highly decreased in such intervals and sometimes reaches zero. As a result of the current research, it is concluded that production of this reservoir is extremely dependent on possible fractures. Fractures aperture was measured in accordance with Luthi and Souhaite (1990) technique. It calculates the fracture aperture from resistivity images using the following method:

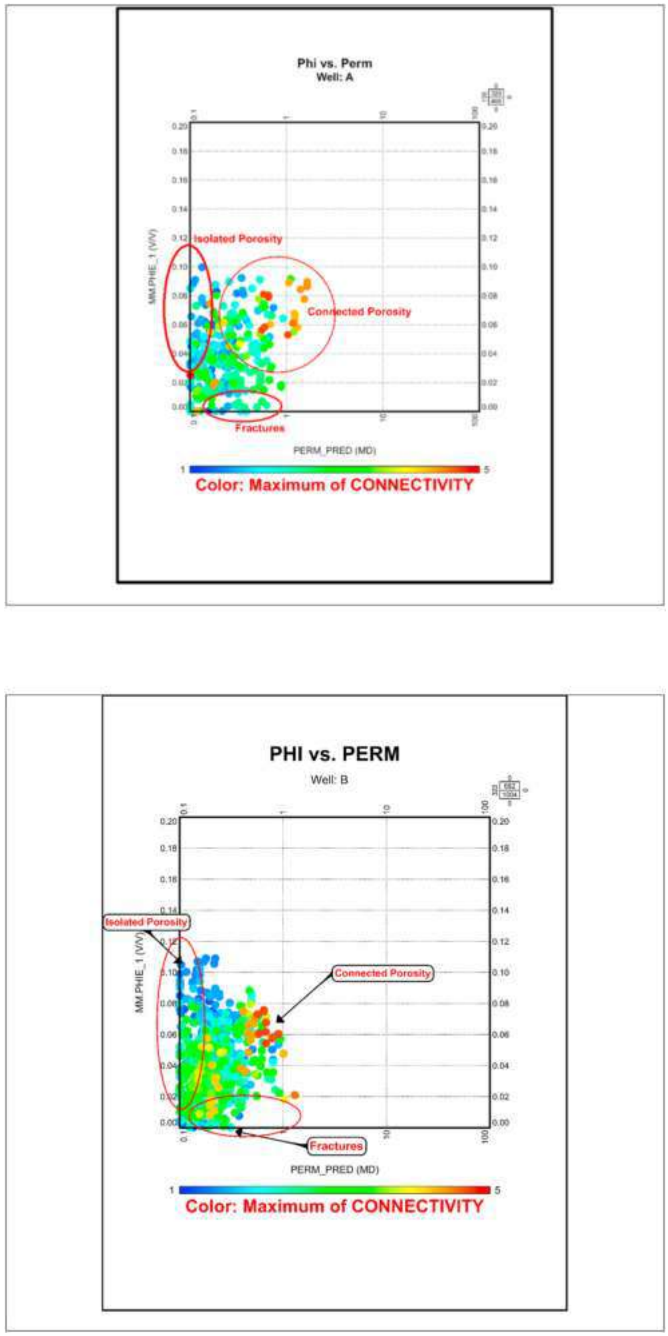

Fig. 6. Calculated connectivity log is indicated by color on POR-PERM cross-plots in 2 selected wells. (For interpretation of the references to color in this figure legend, the reader is referred to the Web version of this article.)

$$\text{Fracture width} = c * A * (\text{Rmf}^\wedge b) * \text{Rxo}^\wedge(1 - b)$$

Parameters c and b are constants and A represents excess current integral. Rxo and Rmf represent resistivity of invaded zone and resistivity of mud-filtrate respectively. Calculated fracture aperture is shown in Fig. 11 which implies the maximum of 12 mm to minimum of 2.5 mm in fracture aperture width. The average of calculated open fracture aperture in this case is equal to 5 mm. It should be noted, the recorded trend of available open and close fractures is also consistent with Zagros trend and it seems they followed the same stress system.

7. Connectivity prediction (ANN method)

In this part, thin section based connectivity logs of two wells were propagated across the field (available wells) by using Artificial Neural Network (ANN). Linqi Zhu et al. (2020) used logging evaluation procedure using multiple overlapping methods integrated with semi-supervised deep learning. Conventional well logs and their relations with each other were the main input data to estimate connectivity log in those wells lack thin section. The result was plotted on available poro-perm cross-plots and showed good consistency with permeability, porosity and thin section based connectivity log. As it is clear on Fig. 12, pores with low grade of connectivity are marked by dark blue color which mostly show high porosity with low permeability.

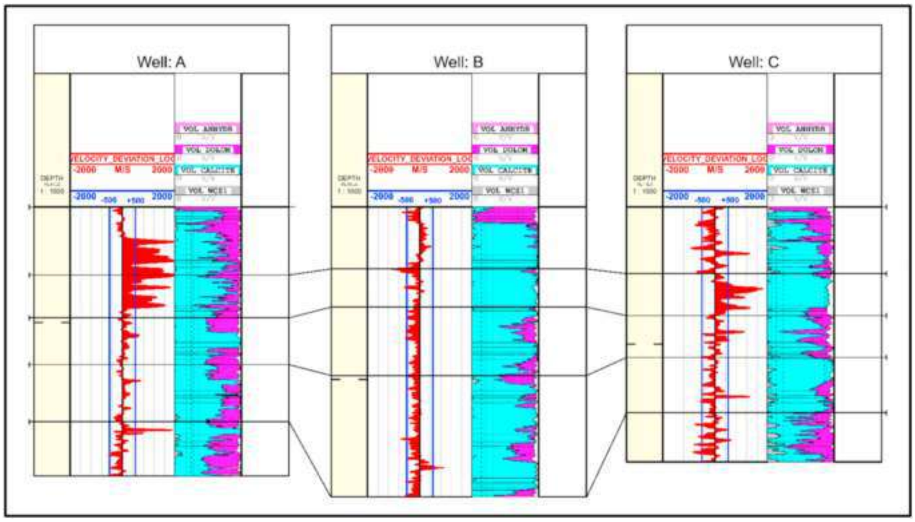

Fig. 7. Velocity deviation log (VDL) estimated in Oligo-Miocene Formation (scale 1/1000).

They are good evidences of available isolated pores (such as moldic, vuggy, micro-porosity) which do not participate in production. High permeability-low porosity area is most often relevant to possible fractures and micro-fractures. Eventually, it was decided to implement a comprehensive distribution on estimated connectivity using seismic data (seismic attributes) throughout the field which gives a comprehensive viewpoint for future field development plans.

8. Connectivity seismic model construction

The prediction of connectivity distribution on reservoir layers in this field is conducted using the Emerge program in Hampson-Russell software. A relationship was extracted between the connectivity logs and seismic data using well logs and 3D seismic data. Then linear transforms were applied between a group of seismic attributes (internal and external) and the target connectivity log. This relationship is used to estimate the connectivity volume at all locations of the seismic volume in reservoir layers. Finally, the obtained connectivity is compared to the connectivity in the location of the blind well, and the results are discussed. For this purpose, 4 wells containing connectivity logs have been selected. However, the data related to 3 wells are applied in the current study to examine the validation. As mentioned earlier, the connectivity data of the last well is used to control work quality.

Using seismic modeling or rock physics, a physically justifiable relationship between a seismic attribute and the well log property can be inferred (Kalkomey, 1997).

The main purpose of this integration is to extend the well log data, which have high vertical resolution, into the spatial volume imaged by the dense three dimensional seismic data, which have low vertical resolution (Whittle, 2016).

According to the workflow shown in Fig. 13, at first, based on the sonic logs and density in 4 wells, the post-stack seismic inversion was performed by the model-based method, and acoustic impedance was obtained. Fig. 14 shows time slice of Acoustic impedance. Also for a better understanding of AI distribution, an arbitrary line which crosses all wells has been shown in Fig. 15.

To validate the results, quality control of the post-stack inversion process is performed. For this purpose, the extracted acoustic impedance from seismic is compared to real acoustic impedance from wells (as mentioned earlier, four wells were used for post-stack inversion, 3 well were used as train and 1 well was as blind well), these comparisons are illustrated in Fig. 16.

For quantitative evaluation, a cross-plot between acquired Acoustic Impedance (AI) and real AI from wells has been shown in Fig. 17. This cross-plot shows that the Cross Correlation between estimated and real AI is about 81% which is a high confident value for this prediction.

After loading the connectivity data in the existing wells, a cross-plot is drawn between them to determine the correlation between the connectivity logs and the acoustic impedance obtained from the post-stack inversion process. Fig. 18 shows the connectivity and Acoustic Impedance cross-plot as a single attribute in 3 of available wells.

The next step is to use several seismic attributes to predict the connectivity with more accuracy.

At this stage, an important parameter is the maximum number of attributes to use. In this part of the analysis, Emerge searches for groups of attributes that can be combined to predict the target. It does this by a process called step-wise regression. This means that it first searches for the single attribute from the list that predicts best by itself.

Here, the maximum number of attributes used is seven and operator length is one, which have been selected with a stepwise-regression approach (Fig. 19).

After the selection of four attributes as the final attributes (1/(Inverted_Model_Zp), Derivative Instantaneous Amplitude, Amplitude Weighted Frequency, Derivative) a cross-plot between the connectivity logs in understudied wells is drawn applying the four selected attributes to check the correlation (Fig. 20). As expected, the correlation has increased compared to the single attribute. The purpose of selecting multiple attributes instead of single attribute is to increase the accuracy of connectivity prediction.

Finally, multiple attributes regression was selected to predict connectivity from seismic data. After using the mentioned method, a connectivity cube was created. A Time slice of this connectivity cube is shown in Fig. 21.

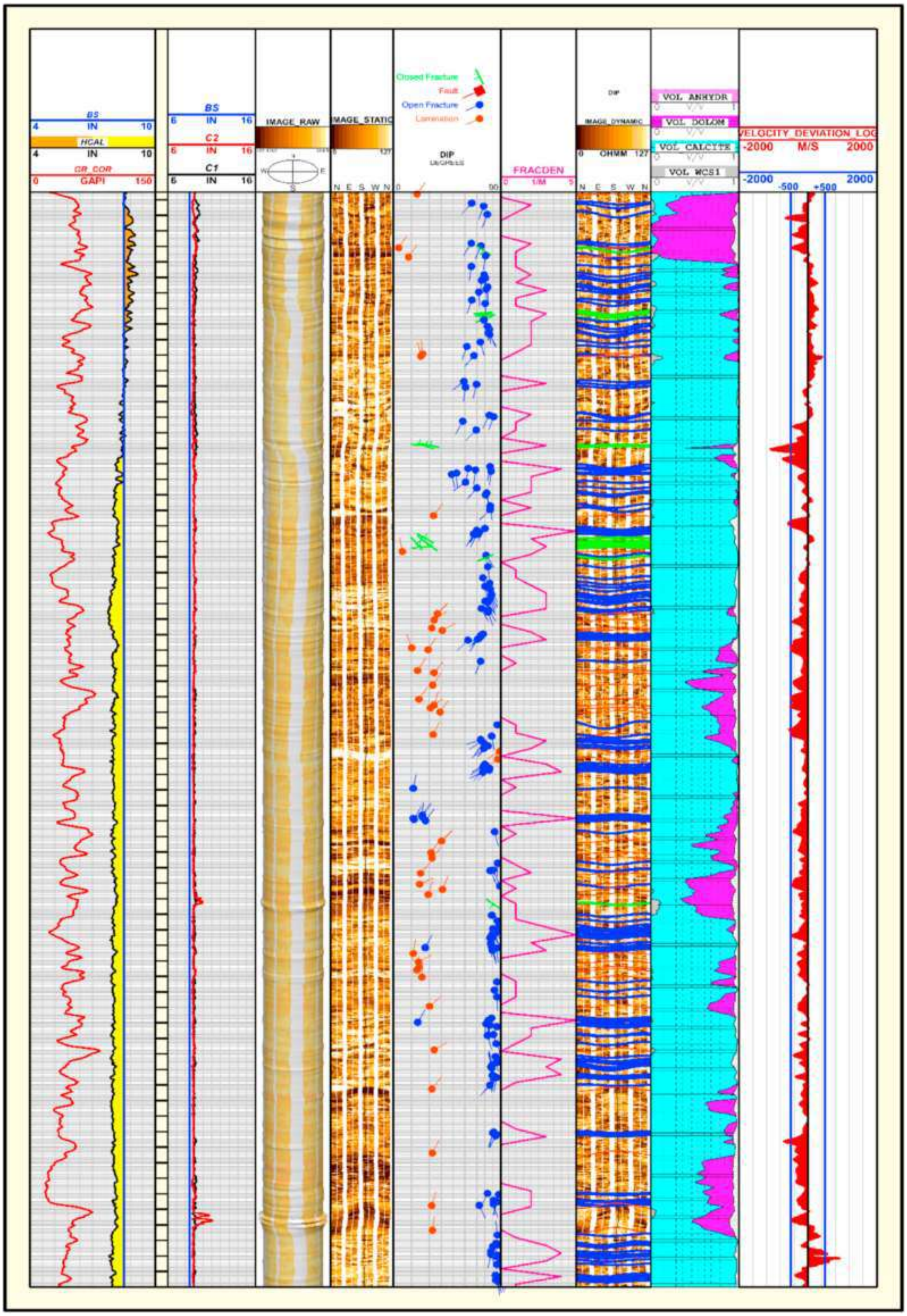

Fig. 8. Image log analysis of well B, Oligo-Miocene carbonates (depth scale 1/300).

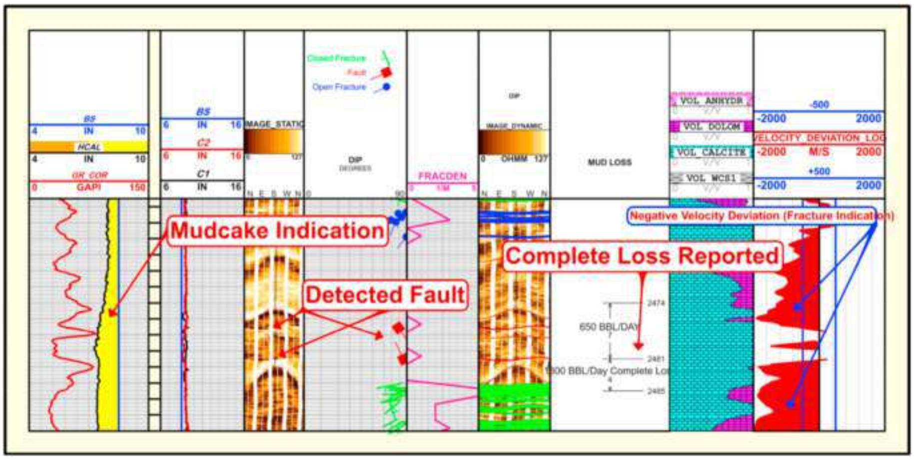

Fig. 9. Possible fault indications, Well B.

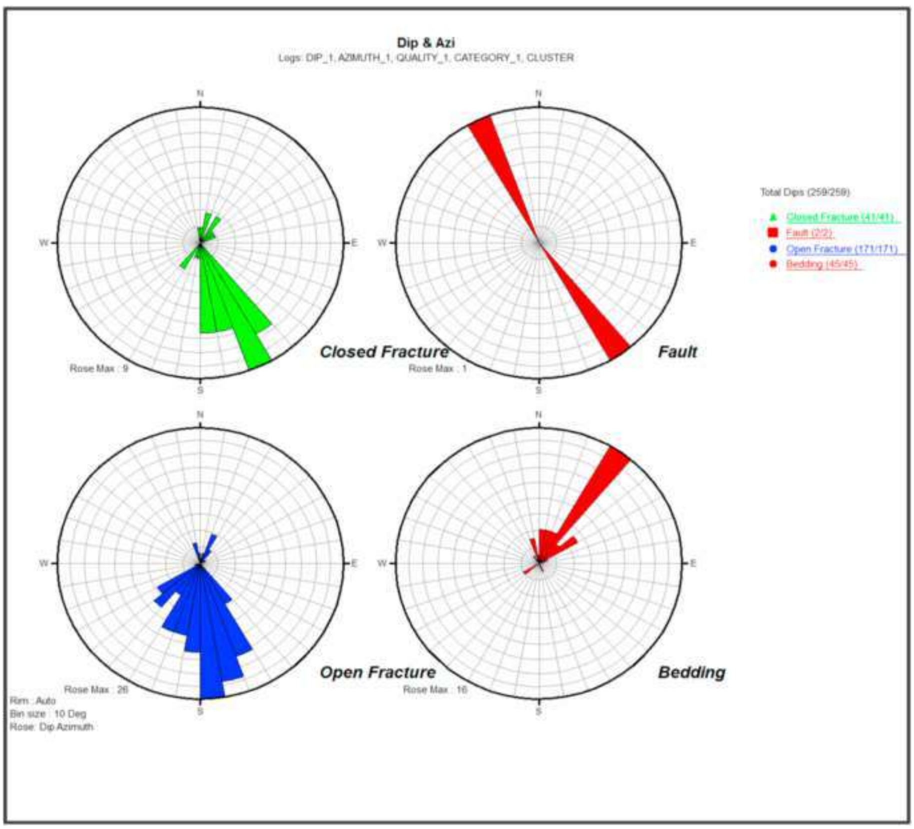

Fig. 10. Rose diagrams illustrating the azimuth and dip of beddings, faults, open and close fractures in well B.

9. Discussion

Measurement of connected porosities and their relationship with production have always been a challenge for geologists and petrophysicists. The intended field was comprehensively studied in terms of pore and fracture characteristics. Thin section analysis, permeability, log porosity, estimated VDL plus image log analysis gave us a comprehensive information on the types of pores, their predominant type, the matrix connection limits, and the involvement of fractures in field production. From this information, it is concluded that the matrix porosity connection is very low. The porosity recorded by neutron, sonic, and bulk density logs is dominantly related to micro-pores. Zero velocity deviation and thin sections were the strong proof of its domination across the field. The pervasive low permeability is another factor that verified the existence of isolated pores in a clean carbonate and it is worth mentioning that its values rarely exceed 1 millidarcy. There are different permeability values recorded on identical geological facies. Nevertheless, these rare and sporadic increases can be directly attributed to fractures. FMI information proved that the studied field is intensively fractured and this is the reason why permeability has occasionally increased in core samples and such increases sometimes even observed in zero porosities. Existence of fault could be another factor amplifying this supposition. It is proved by image log, mud-loss, mudcake and velocity deviation log data and available fractures which dominantly follow the main fault trend and possibly the same stress system. Available open fractures are various in the aperture size range,

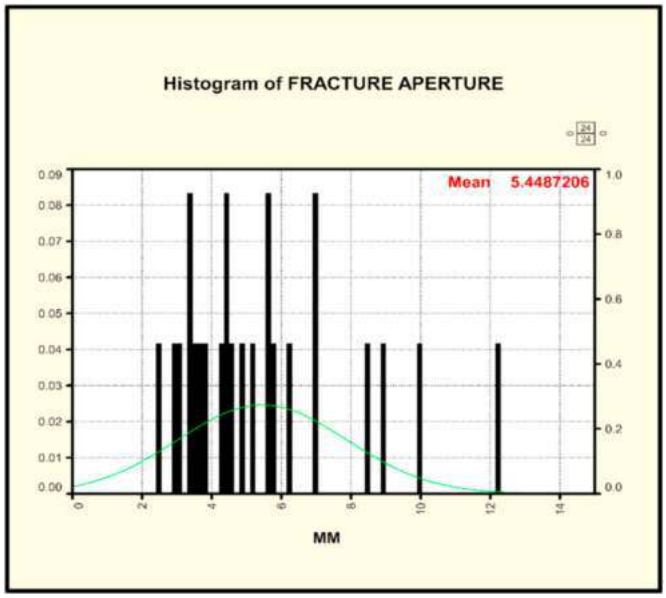

Fig. 11. Histogram of fracture aperture width values which extracted using Luthi and Souhaite (1990) method.

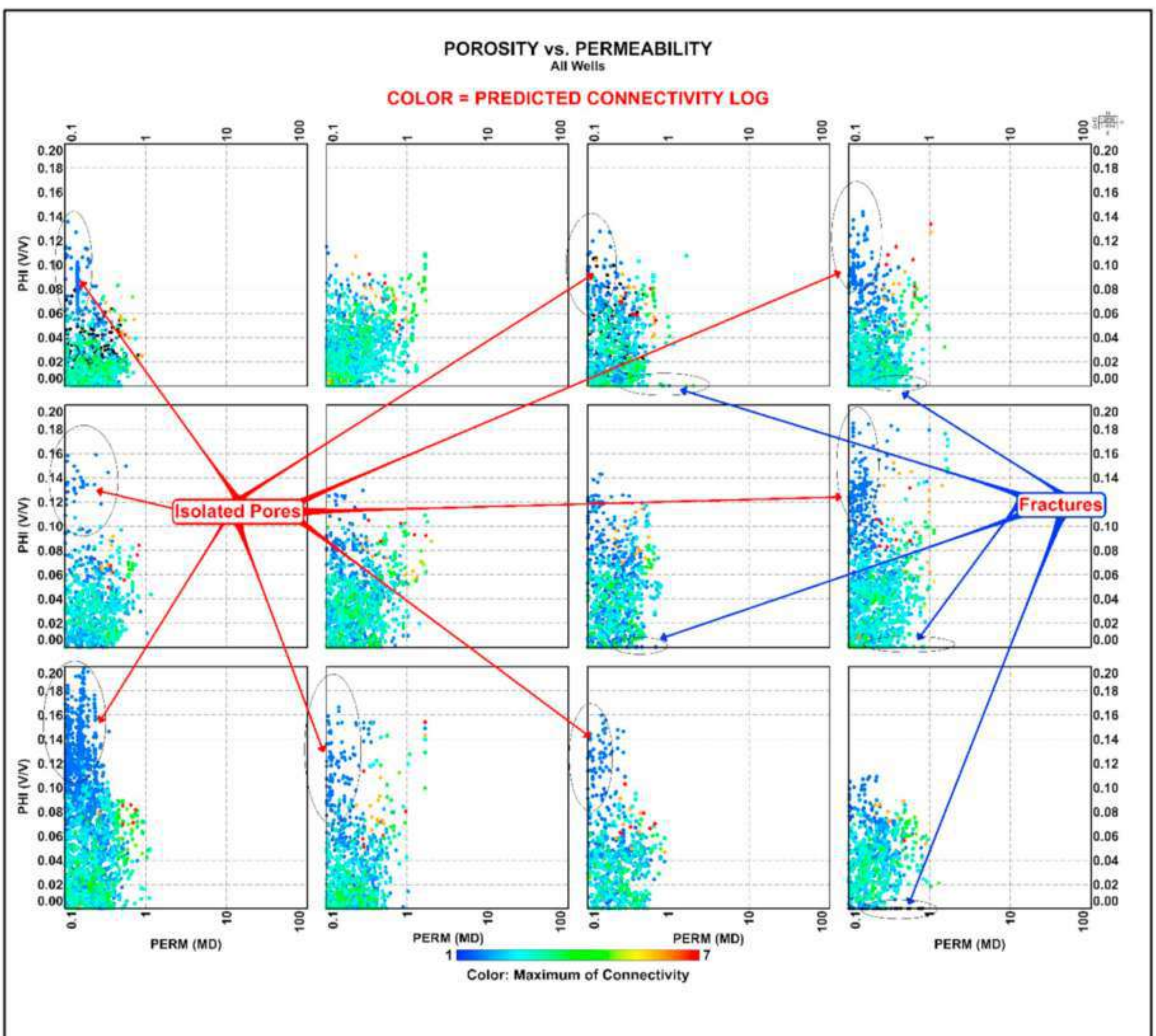

Fig. 12. Estimated connectivity log is shown by color on poro-perm cross-plots. (For interpretation of the references to color in this figure legend, the reader is referred to the Web version of this article.)

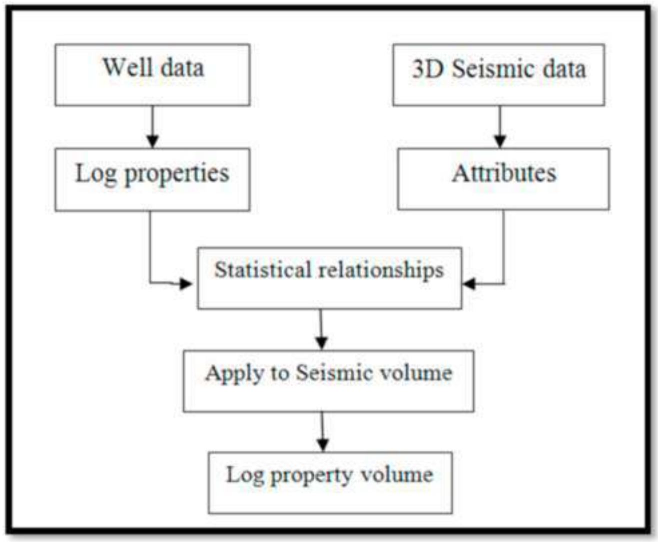

Fig. 13. The general workflow for log property prediction from seismic data.

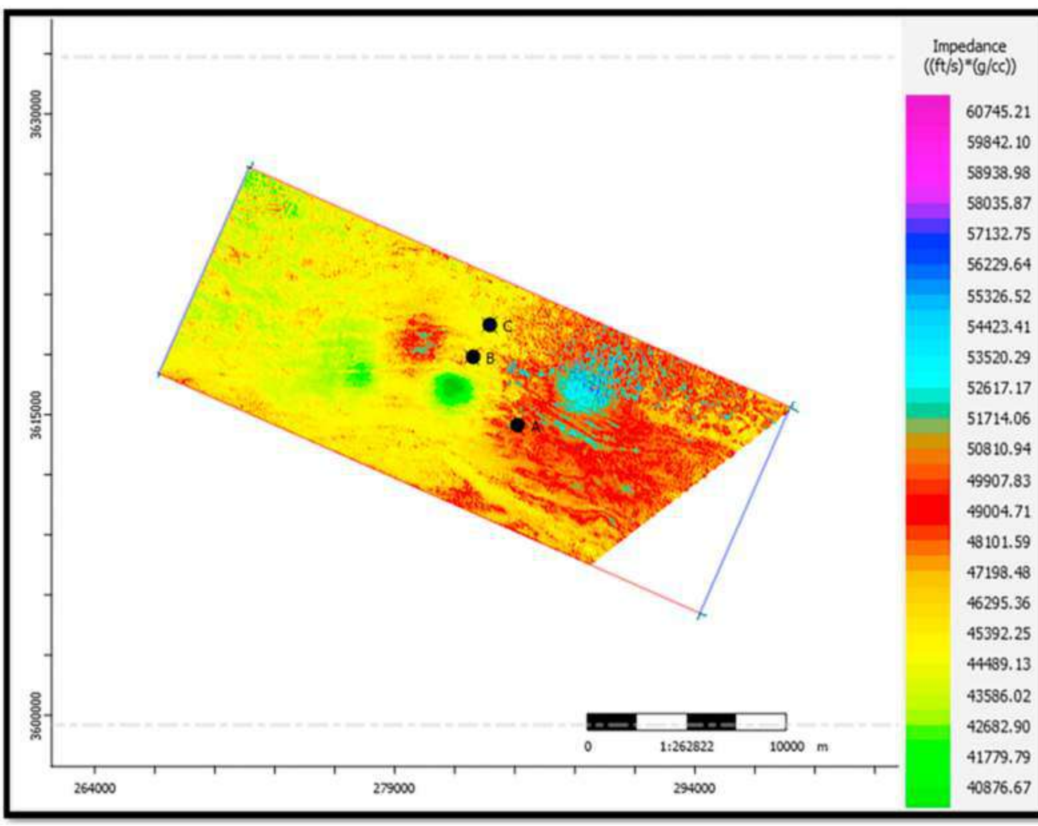

Fig. 14. Time-slice of Acoustic impedance cube and wells location. Color changes indicate different acoustics Impedance. (For interpretation of the references to color in this figure legend, the reader is referred to the Web version of this article.)

so that they differ from micro-size (those are not recorded by FMI and only can be observed on thin-sections) to macro-scale fractures which their calculated aperture width is up to 12.5 mm. Matrix connectivity coefficient which was propagated in all available wells was utilized to construct a comprehensive connectivity 3D model throughout the field with respect to seismic data.

According to the created connectivity cube, the center and west parts of the field have low connectivity values (at the location of wells C and B), but in the east and southeast parts of the field, connectivity has increased gradually (location of well A). In general, connectivity is increasing from the west to the east. There is a green area in the center of the field that indicates less connectivity in comparison with the other areas.

This specific approach could be helpful to propagate the pore

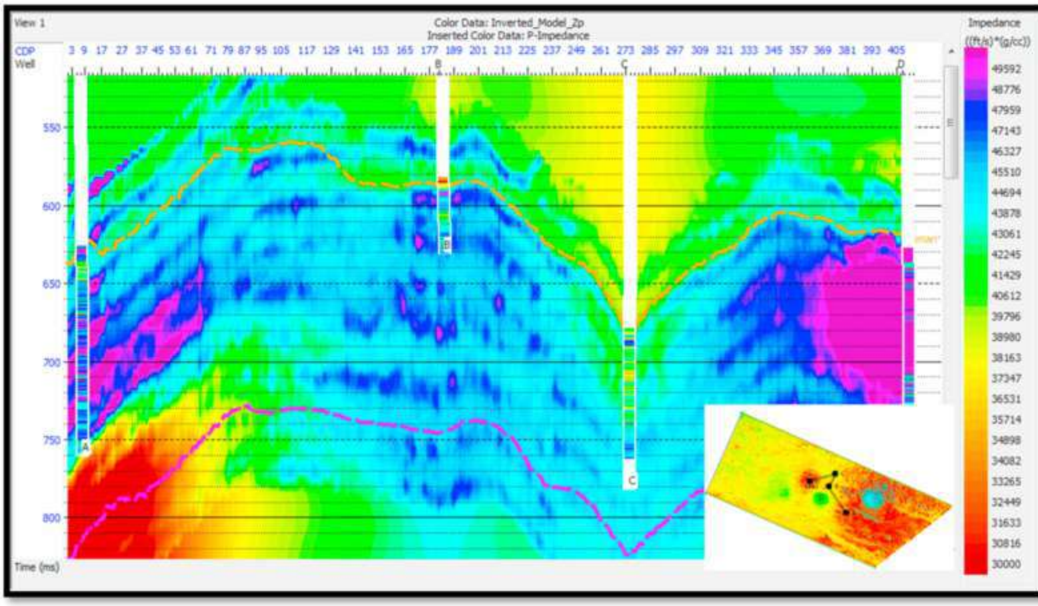

Fig. 15. Arbitrary Line along wells A, B, C, D showing AI distribution through 3D cube.

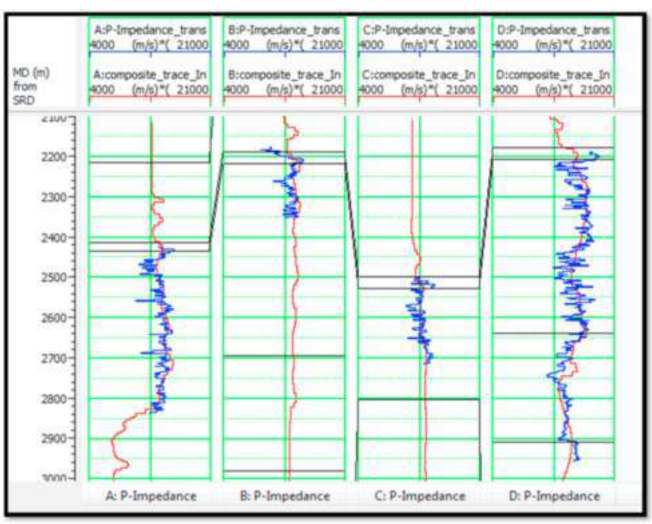

Fig. 16. Comparison of Inverted P-Impedance (red) with the computed P-Impedance log (blue) for wells (A, B, C, D). (For interpretation of the references to color in this figure legend, the reader is referred to the Web version of this article.)

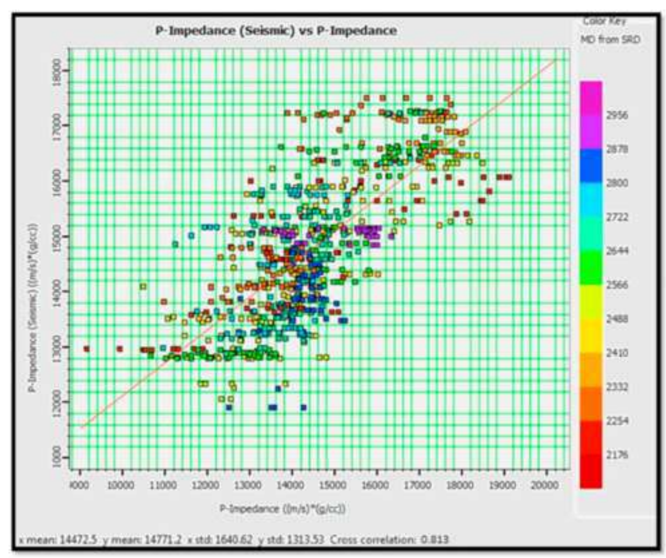

Fig. 17. Cross plot of AI of seismic inversion versus computed AI log (in time) - Cross Correlation = 0.813.

connectivity in the fields containing core analysis, well-log and seismic data.

10. Conclusion

A comprehensive study on Oligo-Miocene carbonate rocks made it clear that its production is dependent on several geological events which are related to sedimentation, diagenesis and tectonics of the area. There are two main factors controlling the permeability values including connected pores and fractures. Although matrix connectivity is generally low as the result of destructive cementation processes, compaction and micro-pore domination, its effect on reservoir permeability must not be ignored. Limy, anhydritic and dolomitic cements in the form of pore blocking, rimming and meniscus have intensively covered the reservoir rock. Along with pore connection, sporadic abundance of fractures has drastically increased the permeability and it can be observed in the samples with low matrix pore connection rate. In addition, high porosity volume samples with low level of permeability are specific evidences of isolated pores. Velocity deviation log (VDL) was also calculated in four of the available wells to validate the pore types domination. Zero velocity deviation across the Asmari reservoir implies that micro-pores are predominantly expanded in this formation. Frequency and aperture size of fractures which have been determined on the available image log confirmed that the understudied reservoir is highly fractured and the aperture width varies from microscale (<50 μm) to 12.5 mm. The density of fractures is increased up to 2 per meter and it is very consistent with mud-loss information such that a complete loss was

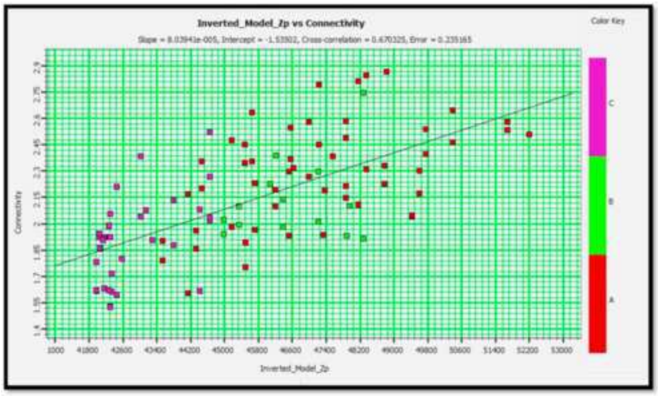

Fig. 18. Cross-plot of Connectivity vs. Acoustic impedance, Colors are coded per well. Cross-correlation = 0.67. (For interpretation of the references to color in this figure legend, the reader is referred to the Web version of this article.)

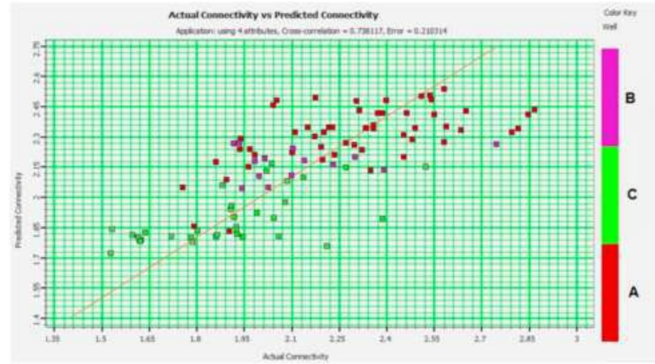

Fig. 20. Cross-plot of Actual vs. Predicted Connectivity, Colors are coded per well. Cross-correlation = 0.738. (For interpretation of the references to color in this figure legend, the reader is referred to the Web version of this article.)

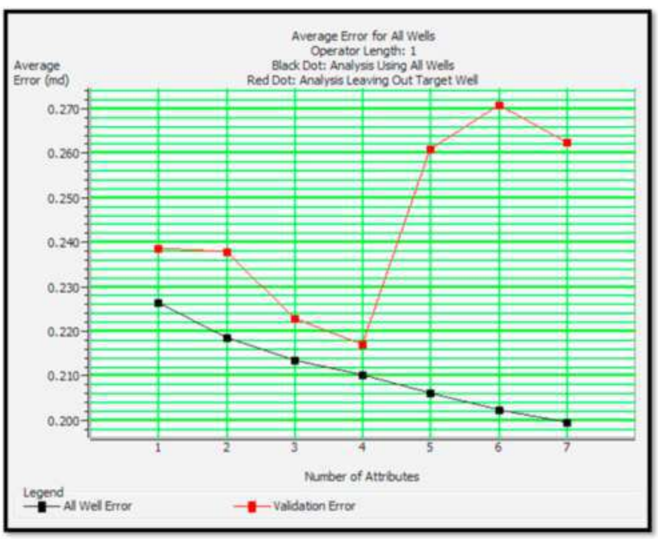

Fig. 19. Average Error versus Number of Attribute. The maximum number of attributes = 7 and operator length = 1.

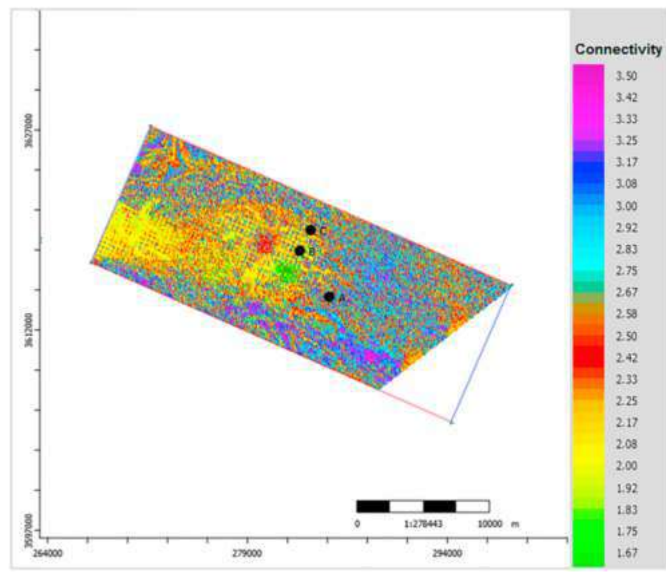

Fig. 21. Time-slice of connectivity cube and wells location. Color changes indicate different connectivity. (For interpretation of the references to color in this figure legend, the reader is referred to the Web version of this article.)

reported in the identified faulty zone. Detected fractures obviously follow the main Zagros fault trend (NW-SE). Finally, calculated connectivity was predicted in other wells using Artificial Neural Network (ANN) and a 3D model was constructed with respect to seismic attributes. For this purpose, in the first step, AI cube was acquired via model-based inversion method. The validation of estimated AI has been tested by real value of AI at blind well location. After that, the optimum seismic attributes were obtained by using stepwise regression and eventually, ANN method was used to calculate connectivity throughout of 3D seismic data. Consequently, the results give a precise perspective of pore connection distribution throughout the studied field.

Credit author statement

Reza Mohebian: Supervision, Conceptualization, Methodology, Software, Writing- Reviewing and Editing. Shervin Bahramali Asadi Kelishami: Data curation, Writing- Original draft preparation, Software. Omidreza Salmian: Software, Validation.

Declaration of competing interest

The authors declare that they have no known competing financial interests or personal relationships that could have appeared to influence the work reported in this paper.

References

Alavi, M., 2004a. Regional stratigraphy of the Zagros fold–thrust belt of Iran and its proforeland evolution. Am. J. Sci. 304, 1–20.

Alavi, Mehdi, 2004b. Regional stratigraphy of the Zagros fold-thrust belt of Iran and its proforeland evolution. American Journal of Science JANUARY 304. https://doi.org/10.2475/ajs.304.1.1.

Allahkarampour Dill, M., Seyrafian, A., Vaziri-Moghaddam, H., 2010. The Asmari Formation, north of the Gachsaran (Dill anticline), southwest Iran: facies analysis, depositional environments and sequence stratigraphy. Carbonates Evaporites 25, 145–160. https://doi.org/10.1007/s13146-010-0021-6.

Anselmetti, Flavio S., Gregor, P., 1999. The Velocity-Deviation Log tool to predict pore type and permeability trends in carbonate drill holes from sonic and porosity or density logs. AAPG Bull. 83 (3), 450–466.

Berberian, M., 1995. Master "blind" thrust faults hidden under the Zagros folds: active basement tectonics and surface morphotectonics. Tectonophysics 241, 193–224.

Cook, J., Growcock, Frederick, Guo, Q., Hodder, Michael, van Oort, Eric, 2011. Stabilizing the wellbore to prevent lost circulation, 23, 26–35.

Ehrenberg, Stephen, Eberli, Gregor, Baechle, Gregor, 2006. Porosity–permeability relationships in miocene carbonate platforms and slopes seaward of the great barrier reef, Australia (ODP leg 194, marion plateau). Sedimentology 53, 1289–1318. https://doi.org/10.1111/j.1365-3091.2006.00817.x.

El Husseiny, Ammar, Vanorio, Tiziana, 2017. Porosity-permeability relationship in dual-porosity carbonate analogs. Geophysics 82, MR65–MR74. https://doi.org/10.1190/geo2015-0649.1.

Google earth V 7.3.3.7786, 2020. Khuzestan, Iran. Sep 19.

Hampson, D., Schuelke, J., Quirein, J., 2001. Use of multi-attribute transforms to predict log properties from seismic data. Geophysics 66 (1), 220–236.

Heydari, E., 2008. Tectonic versus eustatic control on supersequences of the Zagros Mountains of Iran. Tectonophysics 451, 56–70.

James, G., Wynd, J., 1965. Stratigraphic nomenclature of Iranian oil consortium agreement area. AAPG Bull. 49, 2182–2245.

Kalkomey, C., 1997. Potential risks when using seismic attributes as predictors of reservoir properties. Lead. Edge 16 (3), 247, 1997.

Kelishami, S.B.A., Mohebian, R., 2021. Petrophysical rock typing (PRT) and evaluation of Cenomanian–Santonian lithostratigraphic units in southwest of Iran. Carbonates Evaporites 36, 13. https://doi.org/10.1007/s13146-020-00669-3.

Lima, M.C.O., Pontedeiro, E.M., Ramirez, M., et al., 2020. Petrophysical correlations for the permeability of coquinas (carbonate rocks). Transport Porous Media 135, 287–308. https://doi.org/10.1007/s11242-020-01474-1.

Luthi, S.M., Souhaite, P., July 1990. Fracture apertures from electrical borehole scans. Geophysics 55 (7).

Mazzullo, S., 2004. Overview of porosity evolution in carbonate reservoirs. Kansas Geological Society Bulletin 79.

Raymond Carl, Murray, 1960. Origin of porosity in carbonate rocks. J. Sediment. Res. 30 (1), 59–84. https://doi.org/10.1306/74D709CA-2B21-11D7-8648000102C1865D.

Schlumberger, 2015. Wireline Services Catalog (Houston, Texas).

Stampfli, G., Marcoux, J., Baud, A., 1991. Tethyan margins in space and time. Palaeogeogr. Palaeoclimatol. Palaeoecol. 87, 373–409.

Tavakoli, Vahid, 2019. Carbonate Reservoir Heterogeneity: Overcoming the Challenges. https://doi.org/10.1007/978-3-030-34773-4.

Tonietto, Sandra Neils, Smoot, Margaret Z., Pope, Michael, 2014. Pore type characterization and classification in carbonate reservoirs. AAPG 2014. #41432.

Wang, Boli, Zhao, Xisen, Wen, Zhou, Chang, Bin, Xu, Hao, 2020. Quantitative characterization of pore connectivity and movable fluid distribution of tight sandstones: a case study of the upper triassic chang 7 member, yanchang formation in ordos basin, China. Geofluids 2020, 13. https://doi.org/10.1155/2020/5295490. Article ID 5295490.

Whittle, G., 2016. Master dissertation Uncertainty estimation in the quantitative interpretation of inverted reservoir property volumes. University of Houston.

Zhou, Xueqing, Zhang, Chong, Zhang, Zhansong, Zhang, Renfeng, Zhu, Linqi, Zhang, Chaomo, 2019. A saturation evaluation method in tight gas sandstones based on diagenetic facies. Mar. Petrol. Geol. 107, 310–325. https://doi.org/10.1016/j.marpetgeo.2019.05.022. ISSN 0264-8172.

Zhu, Linqi, Zhang, Chong, Zhang, Chaomo, Zhang, Zhansong, Zhou, Xueqing, Liu, Weinan, Zhu, Boyuan, 2020. A new and reliable dual model- and data-driven TOC prediction concept: a TOC logging evaluation method using multiple overlapping methods integrated with semi-supervised deep learning. J. Petrol. Sci. Eng. 188, 106944. https://doi.org/10.1016/j.petrol.2020.106944.